HHS Public Access

Author manuscript

Eur J Oral Sci. Author manuscript; available in PMC 2019 October 01.

Published in final edited form as:

Eur J Oral Sci. 2018 October ; 126(5): 433–436. doi:10.1111/eos.12563.

Inactivation of *Fam20b* in the neural crest-derived mesenchyme of mouse causes multiple craniofacial defects

Xuenan Liu[#1], **Nan Li**[#2], **Hua Zhang**[3], **Jing Liu**[2], **Nan Zhou**[2], **Chunxiao Ran**[2], **Xiaoyan Chen**[2], **Yongbo Lu**[3], **Xiaofang Wang**[3], **Chunlin Qin**[3], **Jing Xiao**[2,*], and **Chao Liu**[2,*]

[1]Department of Radiology, The 2nd Hospital Affiliated to Dalian Medical University, Dalian, Liaoning, China

[2]Department of Oral Pathology, College of Stomatolgy, Dalian Medical University, Dalian, Liaoning, China

[3]Department of Biomedical Sciences and Center for Craniofacial Research and Diagnosis, Texas A&M University College of Dentistry, Dallas, TX, USA

[#] These authors contributed equally to this work.

Abstract

The glycosaminoglycan (GAG) chains attached to the core proteins of proteoglycans (PGs) exert multiple roles, such as enriching signal molecules and regulating the binding of ligands to the corresponding receptors. Family with sequence similarity 20 member B (FAM20B), a newly identified kinase, is essential for the formation of GAG chains. FAM20B phosphorylates the initial xylose on the side chain of a serine residue in the protein. Although the GAG chains of PGs are believed to be indispensable during craniofacial development, there were few reports on their exact functions in craniofacial organogenesis. In this study, by mating the *Wnt1-cre* mice with *Fam20b* floxed mice (*Fam20b*$^{f/f}$ mice) mice, we created *Wnt1-Cre;Fam20b*$^{f/f}$ mice in which *Fam20b* was ablated in the neural crest-derived mesenchyme. The *Wnt1-Cre;Fam20b*$^{f/f}$ mice died immediately after birth due to complete cleft palates. In addition to cleft palates, *Wnt1-Cre;Fam20b*$^{f/f}$ mice also manifested tongue elevation, micrognathia, microcephaly, suture widening and reduced mineralization in the calvarium, facial bones and temporal-mandibular joint (TMJ) bones. These findings indicate that the PGs formed through the catalysis of FAM20B are essential to the morphogenesis and mineralization of the craniofacial complex.

Keywords

glycosaminoglycan; kinase; proteoglycan; craniofacial defects; neural crest

Proteoglycans (PGs) are made of core proteins and one or several glycosaminoglycan (GAG) chains; the core proteins and GAG chains may perform distinctive functions (1). The GAG chains not only provide physical elasticity and mechanical supports for tissues or

[*]Chao Liu & Jing Xiao, Department of Oral Pathology, College of Stomatolgy, Dalian Medical University, Dalian, Liaoning, 116044, China cliu@dmu.edu.cn; xiaoj@dmu.edu.cn.

Conflicts of interest- The authors declare that they have no conflicts of interest.

organs, but also regulate intracellular signaling by modulating the affinity of growth factors to receptors (2, 3). The synthesis of the GAG chain is initiated by linking a xylose to the serine residue of a core protein via O-linkage (4). After the subsequent addition of two galactoses onto the xylose, the phosphorylation of the xylose is required for the addition of a gluconic acid (GlcA) to form the tetrasaccharide linkage (GlcAβ1-3Galβ1-3Galβ1-4Xylβ1-O-Ser), which connects GAG chains (disaccharide repeats) to core proteins (5). Loss of phosphorylation in the initial xylose leads to a premature termination of the tetrasaccharide linkage, which impaired the assembly of GAG chains (5, 6). Family with sequence similarity 20 member B (FAM20B) is identified as a kinase responsible for phosphorylating the initial xylose in the tetrasaccharide linkage of GAG chains (7, 8). The *Fam20b*-dependent phosphorylation on the initial xylose is so critical for the formation of tetrasaccharide linkage that the conventional loss-of-function of *Fam20b* results in embryonic lethality in mouse (9), and severe deformities in the cartilages and bones of zebrafish (10). Although we previously reported that inactivation of *Fam20b* in oral ectoderm led to the supernumerary incisors along with the compromised enamel (11), the roles of *Fam20b* in the development of craniofacial mesenchyme remain largely unknown.

All procedures for animal experiments in this study followed the protocol approved by the Animal Care and Use Committee at Dalian Medical University. To create *Wnt1-cre;Fam20b*$^{f/f}$ mice, we first mated the *Wnt1-cre* mice with *Fam20b*$^{f/f}$ mice to produce *Wnt1-cre;Fam20b*$^{fl+}$. Then, we generated *Wnt1-cre;Fam20b*$^{f/f}$ mice by crossing *Wnt1-cre;Fam20b*$^{fl+}$ mice with *Fam20b*$^{fl+}$or *Fam20b*$^{f/f}$ mice. Genotyping was done as previously described (11). We observed that all the *Wnt1-cre;Fam20b*$^{f/f}$ mice died immediately after birth. The *Wnt1-cre;Fam20b*$^{fl+}$ littermates showed no apparent difference from wild type littermates. All the *Wnt1-cre;Fam20b*$^{f/f}$ mice exhibited a reduction of cranial size (microcephaly) with the particularly shortened mandible (micrognathia) and nose (Fig. 1A&B). As a result of micrognathia, the fronto-naso-mental (FNM) angle in *Wnt1-cre;Fam20b*$^{f/f}$ newborns was reduced to 92^0 (SD=2^0) compared to the angle of 107^0 (SD=5^0; $p<0.05$) in the normal littermates (Fig. 1C&D). The complete cleft palates were detected in all the *Wnt1-cre;Fam20b*$^{f/f}$ newborn mice, which was believed to be the cause of lethality (Fig. 1E&F). Histological analysis further revealed that the tongue position of the E14.5 *Wnt1-cre;Fam20b*$^{f/f}$ mouse was higher than in the normal controls, particularly in the posterior portion (Fig. 1G&H). Our previous study showed that when *Fam20b* was inactivated in the palatal mesenchyme, but not in the mandibular bones by *Osr2-cre*, the palatogenesis in *Osr2-cre;Fam20b*$^{f/f}$ mice was normal (12). Therefore, we speculate that the cleft palates in *Wnt1-cre;Fam20b*$^{f/f}$ newborns were most likely secondary to the micrognathia. Taken into account of the tongue elevation, which seemed to have blocked the elevation of the palatal shelves, there was a strong indication that Pierre Robin Sequence had occurred in the *Wnt1-cre;Fam20b*$^{f/f}$ mice. At the E14.5, although the mesenchyme of the presumptive *Wnt1-cre;Fam20b*$^{f/f}$ tempomandibular joint (TMJ) was evidently condensed, but smaller in size (Fig. 2A&B). The presumptive disc of the *Wnt1-cre;Fam20b*$^{f/f}$ TMJ was hard to be distinguished from the underlying condyle, compared to the wild type (WT) controls (Fig. 2A&B). At E16.5, when the disc was separated from the condyle in the WT control, the *Wnt1-cre;Fam20b*$^{f/f}$ mouse disc was still connected to the condyle by the sustained fibrous tissues (Fig. 2C&D). In addition, the hypertrophic chondrocytes in the

Wnt1-cre;Fam20b$^{f/f}$ condylar cartilage were almost absent, indicating the maturation of the chondrocytes was impaired by the deficiency of *Fam20b*. Von Kossa staining showed that the TMJ of P0 *Wnt1-cre;Fam20b*$^{f/f}$ mouse displayed not only a decreased mineralization in the condyle, but also a thinner disc although the disk was separated from the condyle (Fig. 2E&F). Since a previous study reported that the abrogation of *Fam20b* in the mesoderm-derived joint cartilage resulted in over-proliferation, poor differentiation and impaired maturation of the chondrocytes (12), our findings in this study suggested that the differentiation and maturation of the chondrocytes in tempomandibular joint, which were derived from neural crest mesenchyme, were also impaired due to *Fam20b* deficiency.

Although microcephaly was evident with a complete penetrance in *Wnt1-cre;Fam20b*$^{f/f}$ newborns, craniosynostosis, characterized with the premature closure of cranial sutures, was not observed. On the contrary, in the *Wnt1-cre;Fam20b*$^{f/f}$ cranium, the anterior and posterior fontanels were connected together by the broadened sagittal suture (Supplemental Fig. 1A&B). Von Kossa Staining confirmed that the sagittal suture between the *Wnt1-cre;Fam20b*$^{f/f}$ parietal bones became enlarged rather than premature closure (Supplemental Fig. 1C&D). Similarly, the mineralized mandibular and palatine bones in the *Wnt1-cre;Fam20b*$^{f/f}$ mice showed the reduced volume, although the morphology of tooth germs looked normal compared to the normal controls (Supplemental Fig. 1E&F). These results indicated that the loss of *Fam20b* could impair the differentiation, maturation and/or mineralization of the osteoblasts during intramembranous ossification.

In this study, we demonstrated that the loss of *Fam20b* impaired the morphogenesis of mandible, the differentiation and maturation of the osteoblasts and chondrocytes derived from neural crest. Since the bones and cartilages in craniofacial region are derived from the neural-crest mesenchyme (13), it is not surprising that abrogation of *Fam20b* in the neural crest cells causes the deformities in craniofacial complex. PGs are distributed throughout cell surface, intracellular, pericellular and extracellular spaces (16, 17), and capable of modulating BMP, HH, FGF and Wnt signaling during development through the GAG chains, which sequester and enrich the factors, and/or facilitate the binding of the factors to the receptors (18, 19, 20, 21). Because the inactivation of *Fam20b* may incapacitate the elongation and assembly of GAG chains in many types of PGs (6, 8), the signaling pathways affected by *Fam20b* loss in various tissues may be different. Therefore, it is hard to conclude that a specific signaling pathway is affected by the loss of *Fam20b* in all deformities. Further studies are needed to clarify how *Fam20b* deficiency results in different types of developmental defects.

Supplementary Material

Refer to Web version on PubMed Central for supplementary material.

Acknowledgement-

This work is supported by NIH grant (DE022549 to C.Q.) and the Natural Science Foundation of China grant (81771055 to C.L.)

References

1. Kjellen L, Lindahl U. Proteoglycans: structures and interactions. Annu Rev BioBiochem. 1991; 60:443–475.
2. Sarrazin S, Lamanna WC, Esko JD. Heparan sulfate proteoglycans. Cold Spring Harb Perspect Biol. 2011; 3: a004952. [PubMed: 21690215]
3. Mikami T, Kitagawa H. Biosynthesis and function of chondroitin sulfate. Biochim Biophys Acta. 2013;1830:4719–4733. [PubMed: 23774590]
4. Prydz K, Dalen KT. Synthesis and sorting of proteoglycans. J Cell Sci. 2000;113:193–205. [PubMed: 10633071]
5. Couchman JR, Pataki CA. An introduction to proteoglycans and their localization. J Histochem Cytochem. 2012;60:885–897. [PubMed: 23019015]
6. Nadanaka S, Zhou S, Kagiyama S, Shoji N, Sugahara K, Sugihara K, Asano M, Kitagawa H. EXTL2, a member of the EXT family of tumor suppressors, controls glycosaminoglycan biosynthesis in a xylose kinase-dependent manner. J Biol Chem. 2013;288:9321–9333. [PubMed: 23395820]
7. Koike T, Izumikawa T, Tamura J, Kitagawa H. FAM20B is a kinase that phosphorylates xylose in the glycosaminoglycan-protein linkage region. Biochem J. 2009;421:157–162. [PubMed: 19473117]
8. Wen J, Xiao J, Rahdar M, Choudhury BP, Cui J, Taylor GS, Esko JD, Dixon JE. Xylose phosphorylation functions as a molecular switch to regulate proteoglycan biosynthesis. Proc Natl Acad Sci U S A. 2014;111:15723–15728. [PubMed: 25331875]
9. Vogel P, Hansen GM, Read RW, Vance RB, Thiel M, Liu J, Wronski TJ, Smith DD, Jeter-Jones S, Brommage R. Amelogenesis imperfecta and other biomineralization defects in Fam20a and Fam20c null mice.Vet Pathol. 2012;49:998–1017. [PubMed: 22732358]
10. Eames BF, Yan YL, Swartz ME, Levic DS, Knapik EW, Postlethwait JH, Kimmel CB. Mutations in fam20b and xylt1 reveal that cartilage matrix controls timing of endochondral ossification by inhibiting chondrocyte maturation. PLoS Genet. 2011;7:e1002246. [PubMed: 21901110]
11. Tian Y, Ma P, Liu C, Yang X, Crawford DM, Yan W, Bai D, Qin C, Wang X. Inactivation of Fam20B in the dental epithelium of mice leads to supernumerary incisors. Eur J Oral Sci. 2015;123:396–402. [PubMed: 26465965]
12. Ma P, Yan W, Tian Y, Wang J, Feng JQ, Qin C, Cheng YS, Wang X. Inactivation of Fam20B in Joint Cartilage Leads to Chondrosarcoma and Postnatal Ossification Defects. Sci Rep. 2016;6:29814. [PubMed: 27405802]
13. Chai Y, Jiang X, Ito Y, Bringas P, Jr, Han J, Rowitch DH, Soriano P, McMahon AP, Sucov HM. Fate of the mammalian cranial neural crest during tooth and mandibular morphogenesis. Development. 2000;127:1671–1679. [PubMed: 10725243]
14. Hao MM, Foong JP, Bornstein JC, Li ZL, Vanden Berghe P, Boesmans W. Enteric nervous system assembly: Functional integration within the developing gut. Dev Biol. 2016;417:168–181. [PubMed: 27235816]
15. Nagy N, Goldstein AM. Enteric nervous system development: A crest cell's journey from neural tube to colon.Semin Cell Dev Biol. 2017;66:94–106. [PubMed: 28087321]
16. Schaefer L. Proteoglycans, key regulators of cell-matrix dynamics. Matrix Biol. 2014;35:1–2. [PubMed: 24871042]
17. Iozzo RV, Schaefer L. Proteoglycan form and function: A comprehensive nomenclature of proteoglycans. Matrix Biol. 2015;42:11–55. [PubMed: 25701227]
18. Shimokawa K, Kimura-Yoshida C, Nagai N, Mukai K, Matsubara K, Watanabe H, Matsuda Y, Mochida K, Matsuo I. Cell surface heparan sulfate chains regulate local reception of FGF signaling in the mouse embryo. Dev Cell. 2011;21:257–272. [PubMed: 21839920]
19. Dejima K, Kanai MI, Akiyama T, Levings DC, Nakato H. Novel contact-dependent bone morphogenetic protein (BMP) signaling mediated by heparan sulfate proteoglycans. J Biol Chem. 2011;286:17103–17111. [PubMed: 21454551]
20. Filmus J, Capurro M. The role of glypicans in Hedgehog signaling. Matrix Biol. 2014;35:248–252. [PubMed: 24412155]

21. Balasubramanian R, Zhang X. Mechanisms of FGF gradient formation during embryogenesis.Semin Cell Dev Biol. 2016;53:94–100. [PubMed: 26454099]

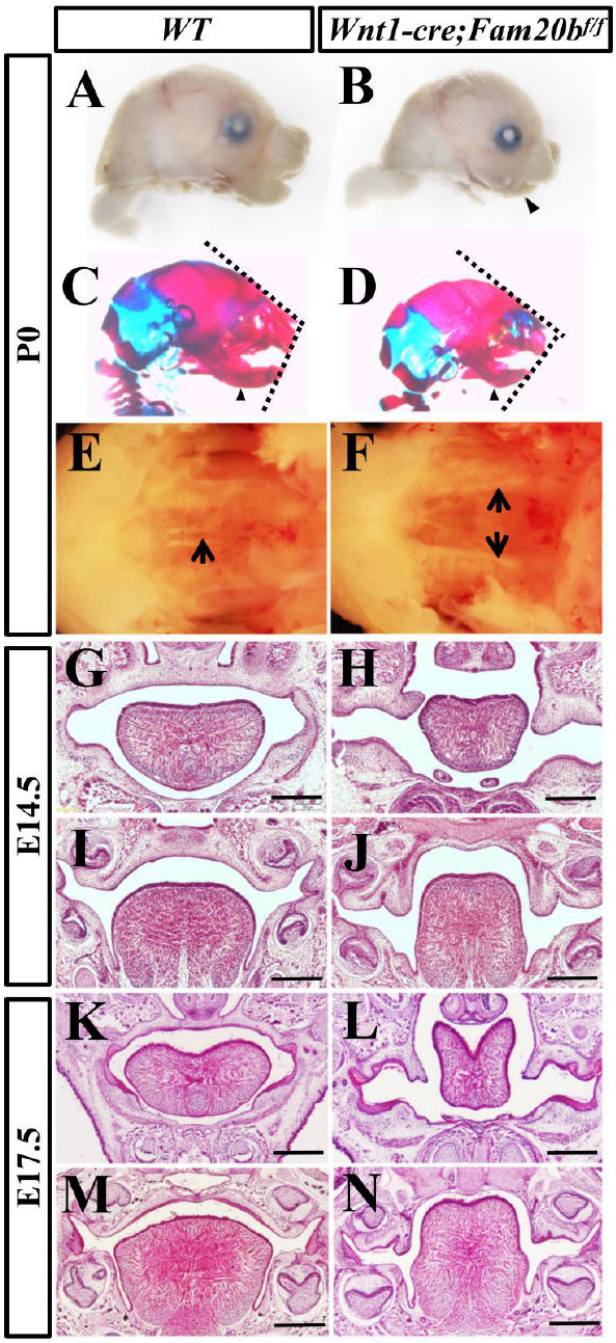

Fig. 1.

Craniofacial morphology of *Wnt1-cre;Fam20b*$^{f/f}$ mice. The gross lateral views for the heads of P0 wild-type (A) and *Wnt1-cre;Fam20b*$^{f/f}$ mice (B), indicating the micrognathia in *Wnt1-cre;Fam20b*$^{f/f}$ mice (arrowhead in B). The bone and cartilage staining showed the micrognathia (arrowhead) and the reduced FNM angle (dashed lines) in the P0 *Wnt1-cre;Fam20b*$^{f/f}$ head (D) compared with the wild-type head (C). The gross ventral view of the upper jaw exhibited a complete cleft palate in P0 *Wnt1-cre;Fam20b*$^{f/f}$ mice (arrows in F) and the integrated palatal shelves in wild-type littermates (E). (G-N) When the palatal shelves in

E14.5 wild-type mouse fused together at both anterior (G) and posterior (I), the palatal shelves of *Wnt1-cre;Fam20b*$^{f/f}$ mouse still separated from each other at anterior (H) and posterior (J). Similarly, compared with the fused E17.5 anterior (K) and posterior palate (M) in wild-type mouse, both the anterior (L) and posterior palatal shelves (N) of *Wnt1-cre;Fam20b*$^{f/f}$ mouse kept vertically. Moreover, the *Wnt1-cre;Fam20b*$^{f/f}$ tongue (J, N) was significantly higher than the wild-type tongue (L, M) at both E14.5 and E17.5. Scale bar, 500um. Three *Wnt1-cre;Fam20b*$^{f/f}$ mouse heads at P0, E14.5 and E17.5, respectively, with the corresponding littermates were used in each experiment.

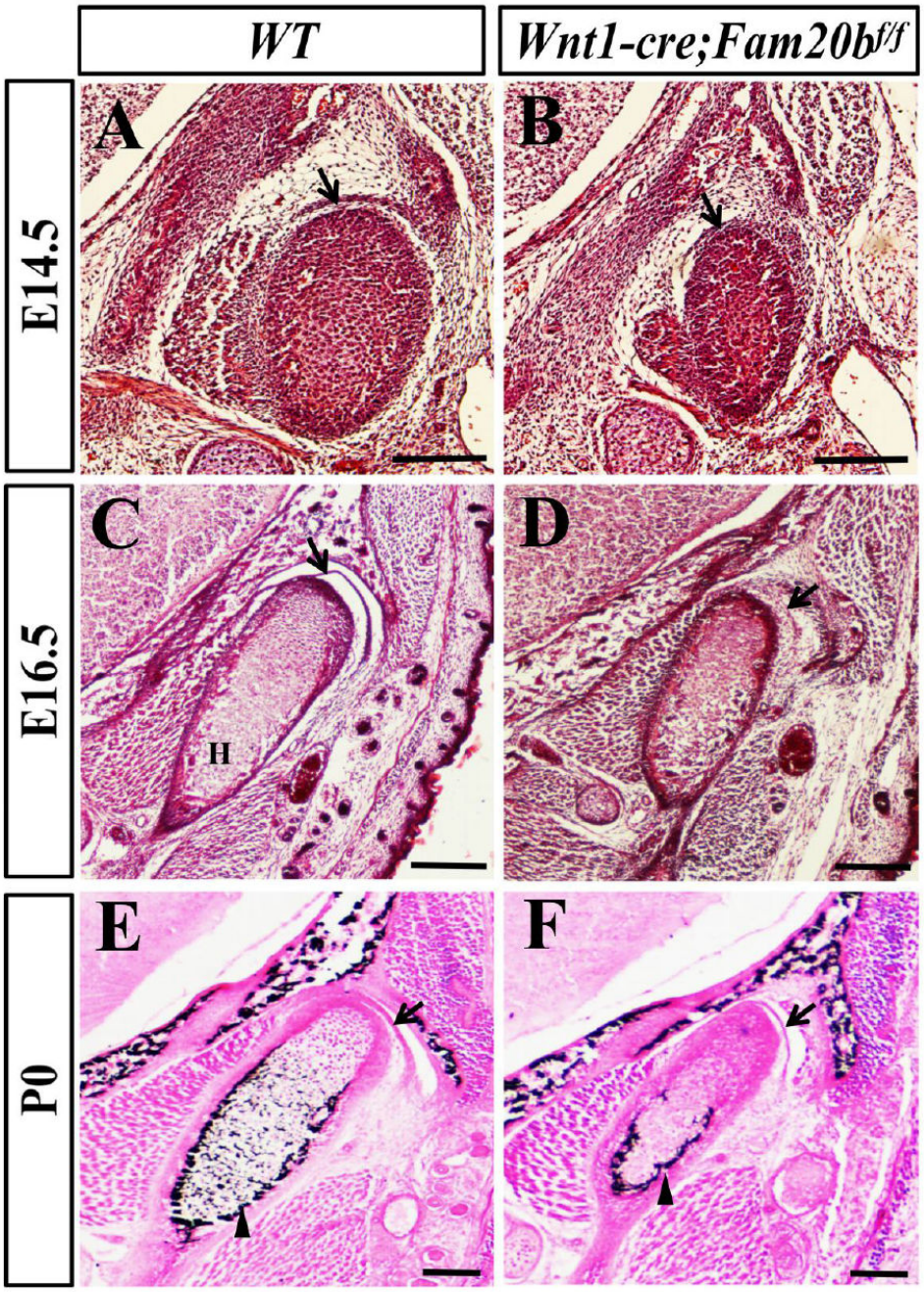

Fig. 2.

The defects in *Wnt1-cre;Fam20b*$^{f/f}$ TMJ. At E14.5, the wild-type mouse displayed a larger presumptive TMJ condensation (A) and a distinct presumptive disc (arrow in A) compared with *Wnt1-cre;Fam20b*$^{f/f}$ mouse (B). At E16.5, the condyle in wild-type mouse separated from the disc (arrow in C) and possessed hypertrophic chondrocytes (H in C), while the *Wnt1-cre;Fam20b*$^{f/f}$ condyle was connected to the disc by fibrous tissue (arrow in D) and devoid of hypertrophic chondrocytes. At P0, although separated, the *Wnt1-cre;Fam20b*$^{f/f}$ disc (arrow in F) was thinner than that in wild-type (E). As shown in Von Kossa staining, the

mineralization in wild-type extended into the condyle (E). In contrast, the mineralization area just surrounded the *Wnt1-cre;Fam20b*$^{f/f}$ condyle (F). Scale bar, 200um. Three E14.5 and P0 *Wnt1-cre;Fam20b*$^{f/f}$ mouse heads were used, respectively, with their littermates in the corresponding experiments. While four E16.5 *Wnt1-cre;Fam20b*$^{f/f}$ heads were employed together with the littermates in the experiments for this figure.